Remote Sensing in Earth Systems Sciences
https://doi.org/10.1007/s41976-025-00229-0

RESEARCH

An Object-Based Crop Classification Using Optimum Remotely Sensed Phenological and Multi-Spectral Data in Pakistan

Wasif Yousaf[1,2] · Sajid Rashid Ahmad[2] · Naeem Shahzad[3] · Amna Ramzan[4] · Ambreena Javaid[5]

Received: 27 January 2025 / Revised: 6 May 2025 / Accepted: 21 May 2025

Abstract

Accurate and timely mapping of crops is essential for water resource management and to ensure sustainable food security. Satellite remote sensing has the well-documented ability to provide crop-type maps based on multispectral temporal datasets. However, due to the highly heterogeneous cropping practices, crop type mapping usually involves large phenological datasets, complex procedures, extensive field data, and resources. Therefore, we developed a simple and efficient image object hierarchy to delineate agricultural field boundaries and identify different crops. The combination of multispectral and temporal profiles was assembled using 23 Landsat 8 images over the period of two cropping seasons in Sahiwal district, Pakistan. The crop calendar information was also used to retrieve unique features distinguishing various crops through rule set development in object-based image analysis (OBIA). The approach incorporated the optimum phenological information at the start, senescence, and peak of the growing season to map major crops (wheat, maize, rice, cotton, sugarcane, orchards, fodder, and other land-cover land-use types including built-up areas, bare soil, grasses, and bushes) in the study area. The overall accuracy for crop maps was reported greater than 84% for both cropping seasons and ranged from 80 to 96% when compared with crop areas, as reported by the agriculture department and through independent accuracy assessment. The proposed workflow not only applies the Earth observation data to generate accurate and reproducible crop and land cover maps but also is an auspicious step to reduce the extensive field work and resources.

Keywords Crop mapping · *NDVI* time series · Crop indices · Object-based image analysis · Phenology

1 Introduction

Food scarcity poses the significant challenges to the populations, particularly in developing and underdeveloped regions [8]. The reality of decreasing water and land resources along with the rapidly growing population demands exploration of possibilities to enhance crop productivity to avoid a food crisis [8]. Therefore, continuous monitoring of crop types and their spatial extent has become an important step toward achieving the milestone of sustainable agricultural yield [40]. The application of remote sensing (RS) and geographic information system (GIS) can lead to the development of accurate crop maps, which can be utilized for crop monitoring and decision-making at local and regional scales [18]. These crop maps are also considered an important parameter for quantifying crop water consumption and crop yield estimation for better water resource management and food security measures [47].

The spatiotemporal variation of vegetation phenology is a well-known indicator for monitoring crop health and for crop classification [7]. Remote sensing and GIS offer state-of-the-art techniques and datasets for delineating temporal and spatial patterns of crop phenology [30]. For this purpose, many recent studies used time-based stacks of vegetation indices in various vegetation-monitoring related studies

✉ Naeem Shahzad
naeem.shahzad@connect.polyu.hk

1 Decision Support System (DSS), Program Monitoring and Implementation Unit (PMIU), Punjab Irrigation Department, Old Anarkali, Lahore, Pakistan

2 College of Earth and Environmental Sciences, Quaid e Azam Campus, University of the Punjab, Lahore, Pakistan

3 Department of Land Surveying and Geo-Informatics (LSGI), The Hong Kong Polytechnic University, Kowloon, Hong Kong SAR, China

4 University Institute of Medical Laboratory Technology (UIMLT), University of Lahore, Lahore, Pakistan

5 Department of Geography, Kinnaird College for Women, Lahore, Pakistan

[4]. A large number of vegetation indices have been defined so far but the most common indicator used for measuring the phenology and health of vegetation is the normalized difference vegetation index (*NDVI*). Most crop mapping studies use temporal stack images or time series of *NDVI* to capture the unique pattern of the phenology cycle of a particular crop and use this pattern as the *NDVI* signature of that crop.

Remote sensing datasets have been widely used in the agricultural domain since the 1970 s when the first Landsat satellite was launched into the Earth's orbit. Compared to manual methods like questionnaires and field surveys, the advantage of remote sensing is the ability to capture a large area quickly, repeat observations over the same area, and require less cumbersome manual work and labor resources. In recent era of advancing computer power and advancements, agricultural mapping methodologies have evolved from single one-time images to multitemporal images acquired from very high-resolution commercial satellites to freely available medium-coarse resolution satellites [19]. Generally, medium to coarse remote sensing images are used in most research due to their free availability and relatively low processing time and computer resources [9]. With all the upcoming and available open data resources and powerful processing and analyzing platforms, there is great potential in fusing optical and radar data for crop-type mapping, which usually involves some complex processing [29].

In addition, the quality of remote sensing data is not the only parameter to obtain efficient results, as the selection of classification technique is also crucial to improving the accuracy of land cover and crop mapping [32]. Object-based image analysis (OBIA) classification algorithm for land cover mapping using optical satellite imagery has drawn notable consideration in recent years. The traditional pixel-based classification algorithms only use spectral characteristics of land features for land cover mapping. In contrast, OBIA not only considers spectral properties of surface features but also utilizes spectral indices, elevation, aspect, meta, and statistical parameters in image classification [3]. Furthermore, OBIA offers better control over the classification process through rule set based classification (X. [24]). The rule set is the sequence of thresholds of multiple spectral and non-spectral (elevation, aspect, shape, position, etc.) characteristics applied to distinguish one land feature from another. A rule set developed for one image to classify it can be used in subsequent temporal images with minor changes, unlike pixel-based conventional supervised and unsupervised classification, which needs to identify spectral signatures each time. Therefore, OBIA can be used as semi-automatic classification algorithm for land cover mapping with minimum repetitive work per image [12].

Crop classification using satellite time series images is not an easy task due to high spatial heterogeneity in cultivation practices, inconsistent availability of satellite images due to environmental conditions, comprehensive processing data, and, most importantly, detailed field surveys to collect training samples during each cropping season [5]. Here, we present an innovative and efficient approach to address these challenges by using temporal crop indices for each crop to avoid complex processing, large volumes of temporal multispectral data, and extensive repetitive field sampling. In this research, the optimal dataset includes temporal crop index (TCI) derived from Landsat 8 *NDVI* stacks and crop calendar information used in OBIA classification for crop type mapping in a semi-automatic manner. We chose OBIA in this study over advanced ML image classification techniques due to OBIA's ability to incorporate spatial, contextual, and multi-type data into the classification process, which provides significant advantages in scenarios where such information is critical. On the other hand, ML techniques are highly effective in applications requiring detailed pixel-level analysis. Keeping the crop classification challenges in mind, the specific objectives of this research included: (a) using optimum remotely sensed data so the methodology can be up-scaled to large areas with minimum processing time and machine resources, (b) ensuring the developed algorithm can be applied to subsequent temporal images with minor changes, and (c) reducing the requirement for field data, which requires extensive resources. Hence, the research methodology can be helpful for crop mapping in a semi-automatic manner with minimum cumbersome processing, dataset, and field sampling data.

2 Materials and Methods

2.1 Description of Study Area

We selected District Sahiwal as the study area, which is located in the Punjab province of Pakistan and comprises a total area of about 3207 km^2 (Fig. 1). Punjab is known as the well-irrigated area, part of the Indus Basin Irrigation System, which is the largest irrigation system in the world [20]. It is situated about 83 km from provincial capital (Lahore) and is the 14 th largest city of the province. According to the Pakistan Bureau of Statistics (PBS), the total agricultural land in the area was about 2800 (87%) km^2 in 2016–2017. Most of the study area is irrigated by underlying unconfined aquifer (groundwater) and canals diverted from the nearby rivers Sutlej and Ravi Rivers. Major crops in the study area include wheat, cotton, maize, potatoes, fodder, and orchards are shown in two cropping seasons, namely Rabi (winter) and Kharif (summer). The Rabi season starts in November and lasts until the end of April the following year, while Kharif season crops are grown from May to the end of October of the same year. Sahiwal is located in the

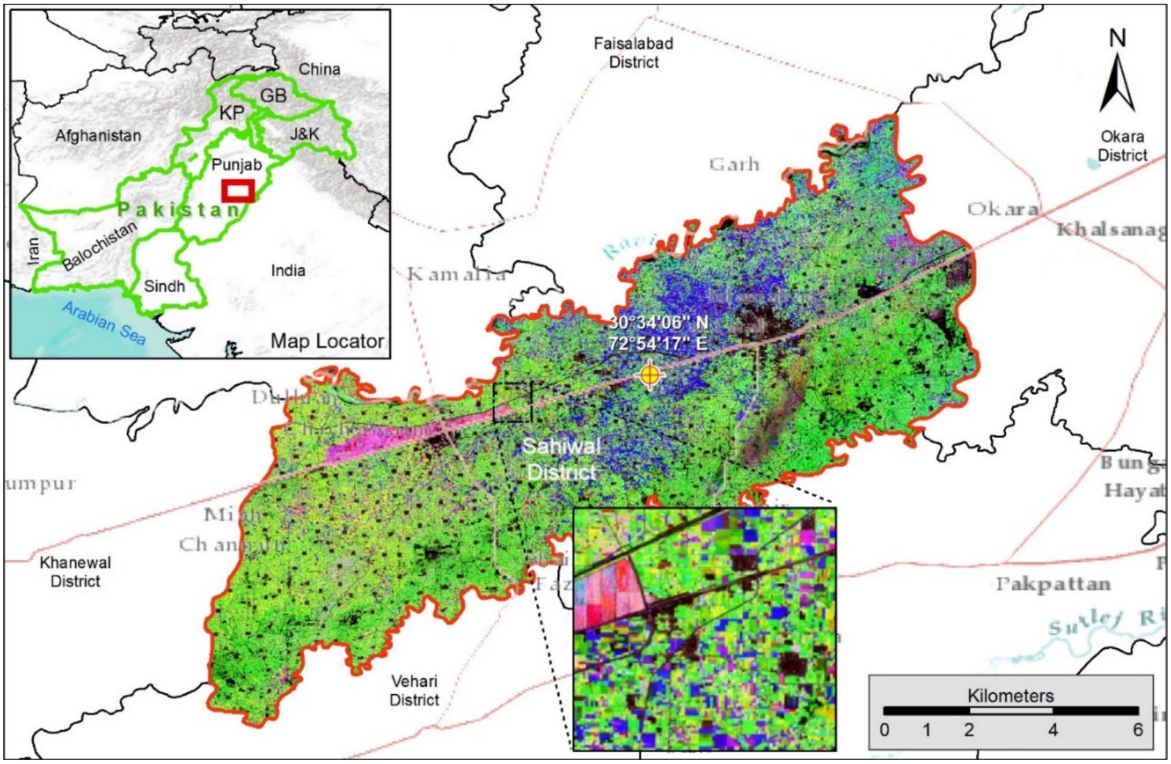

Fig. 1 Location map of the study area (Landsat 8 *NDVI* multi-temporal composite, RGB bands: 22 Nov 2020, 20 Feb 2021 and 15 April 2021)

temperate zone and receives an average rainfall of about 220–370 mm [36].

Wheat is the main crop in the Rabi season, which is usually sown from November to late December. The late or early sowing of wheat depends on the previously planted crop and the weather. Wheat usually reaches the flowering stage in March or April and is finally harvested during May. Besides wheat, other crops, such as potatoes, fodder, and sugarcane, are also sown in the Rabi season, but their cultivation area is much small than that of wheat.

Summer maize, cotton, and rice are the main Kharif crops cultivated in the study area. Kharif maize is cultivated from February to September and harvested until late October. Cotton is usually sown from mid-March to early May, reaching the flowering stage in late July and August and is finally harvested in September. Rice is another important crop, which follows more or less the same crop development stages as Kharif maize, from June to late October. The cropping calendar of all the major crops in the study area cultivated in both seasons is summarized in Fig. 2.

Citrus, mango, and guava orchards are also located in the study area and are considered permanent crops that usually exhibit green reflectance from spring to fall, but their spectral response might be affected by under canopy cover (soil and grass) due to their sparseness. Crops are also sown under the canopy of the orchards in the study area, which also disturbs the pure reflectance of orchards; therefore, we defined a single orchard class in this research. Besides orchards, a small number of vegetables, oil seeds, and sunflowers are also cultivated in the study area. However, due to the relatively small cultivation area, these crops were merged with the grasses/bushes category as the primary concern of the research is to classify major crops. The mean monthly temperatures in the study area range from 12 °C in January to 35 °C in June, and an annual rainfall of 220–370 mm, concentrated primarily in the monsoon season (July–August), influence the phenological cycles of crops, as depicted in Fig. 2. Elevation across the district is relatively consistent, averaging around 170 m asl and thus has minimal impact on cropping patterns.

2.2 Datasets

2.2.1 Satellite Data

Landsat 8 Operational Land Imagery was used as the primary dataset. Atmospherically corrected level 2 surface reflectance (SR) images were acquired from the USGS Earth Explorer online facility. We chose the Landsat archive because of its 30-m spatial resolution, which is sufficient to distinguish different crop fields in

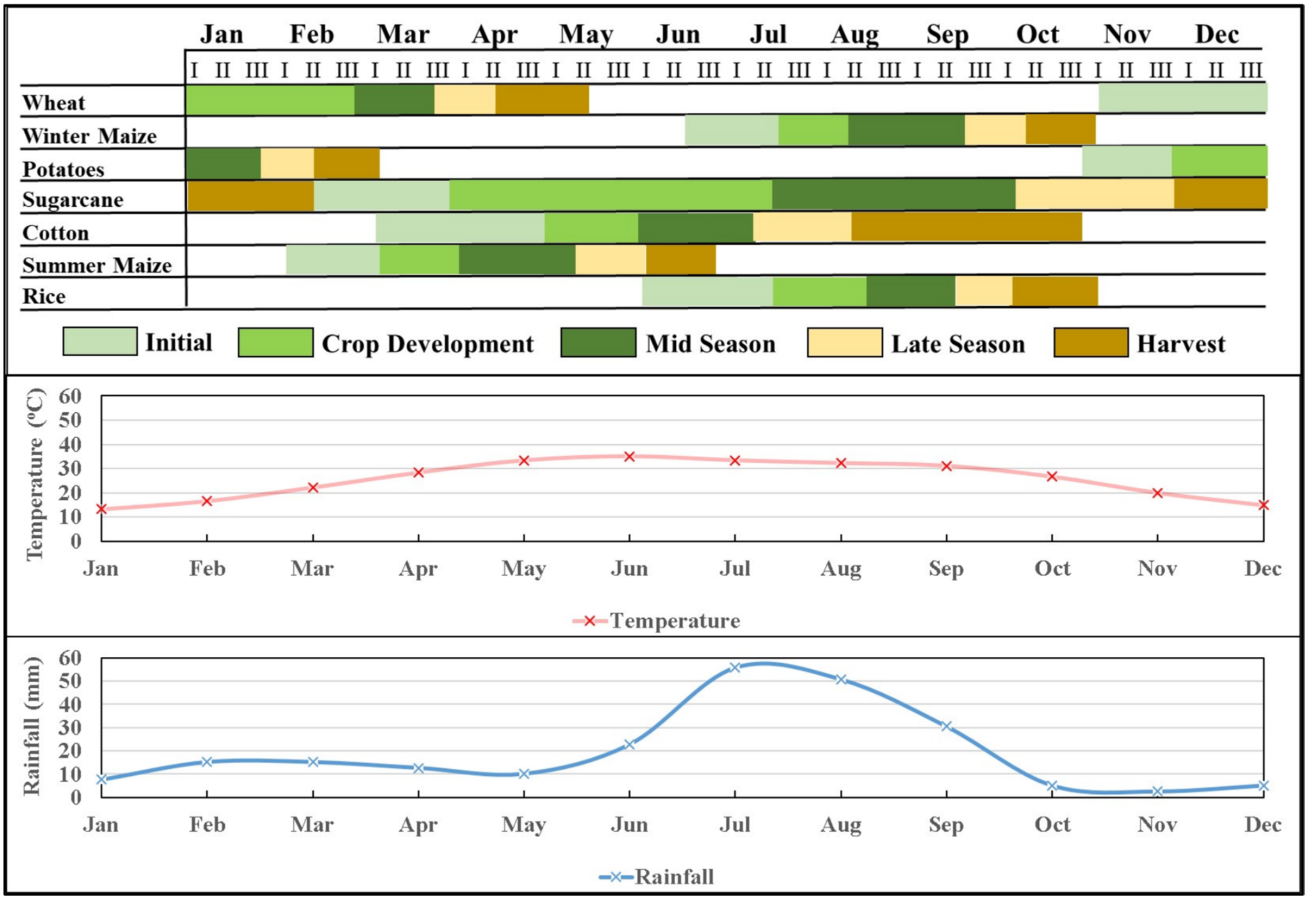

Fig. 2 Crop calendar of major crops in the study area, supplemented with monthly average temperature and rainfall (Source: (Weather [45]))

the study area. Sahiwal District exists in the overlap of two Landsat image coverages (i.e., Row/Path: 149/39, 150/39), meaning four scenes of the study area are available per month. However, all the available Landsat scenes cannot be used due to extreme weather conditions, particularly cloud cover in the study area. Some Landsat spectral bands were not needed in this study due to the research methodology; these bands included band 1 (coastal), band 8 (panchromatic), bands 10 and 11 (thermal), and band 9 (cirrus). The most important bands used in this study were band 4 (red) and band 5 (near-infrared), which were used in the normalized difference vegetation index (*NDVI*). Smoothing filters were also applied to the images to remove the noise and ambiguities in the data due to temporary threshold and saturation conditions of the satellite sensor.

2.2.2 In Situ Data

In situ, crop-type observations were collected from the study area for both cropping seasons through field visits using handheld GPS. These field visits were conducted during the growing period of both cropping seasons. In situ data for the Rabi season were collected from 15 February to 25 March 2021, while Kharif samples were collected from 09 August to 21 September 2021. The samples of all crops were collected through an equally stratified random sampling technique on a daily basis during each field visit. A total of about 600 samples (approximately 50 per crop class) across 12 crop and land cover classes were gathered during field surveys to distinguish non-cropping land cover classes from cropland based on *NDVI* and spectral patterns. The dataset was divided into two subsets: 90% (540 samples) for training and 10% (60 samples) for validation. Based on the focus on performing object-based classification, rather than optimizing a parametric model, and assessing the accuracy of classification, this 90:10 split was selected due to the relatively large sample size and the study's objective of developing an efficient, semi-automatic OBIA classification framework that ensured sufficient data to capture phenological and spectral variability across diverse classes, critical for defining stable OBIA rule sets. The study focused on training a reproducible workflow, which is consistent with similar classification studies employing large field datasets.

For instance, Hao et al. [16] adopted a large training and validation dataset for early crop classification using a pixel-based random forest technique, demonstrating that higher training and validation are required when using a pixel-based parametric classification approach. A foundational work on data splitting, further notes that split ratios should reflect dataset size and study goals [22]. All crop reference data collected from field surveys are represented in Fig. 3.

2.2.3 Crop Reporting Service Data

The Crop Reporting Service (CRS) is a wing of the Punjab Agriculture Department (PAD), which is responsible for estimating the Rabi and Kharif crops every cropping year through its extensive field surveys [1]. At the start of its establishment, the CRS focused on only a few crops to be estimated, but later on other crops were also included due to their growing importance in the development of food security policy and water distribution planning. All crop estimates gathered by the CRS are sent to the Punjab Agriculture Statistics Coordination Board for final publication after approval from the Federal Government. Crop estimates from the CRS are available through the PAD's website (e.g., http://www.agripunjab.gov.pk/crop_reporting) or can be requested from the departmental coordination board. Crop data used in this study to cross-validate the results of the research were obtained from the CRS website [35].

2.3 Methodology

The methodology of the research comprises the following three major steps (i) pre-processing of acquired satellite data, (ii) classification through object-based image analysis (OBIA), and (iii) validation, in which the accuracy of the developed crop maps was assessed as a part of post processing. The overall flow diagram of the research is summarized in Fig. 4.

2.3.1 Pre-Processing

Time series images of remotely sensed datasets underwent several preprocessing procedures before the main analysis and classification. First, we filtered out the atmospherically corrected Landsat Level 2 images for the monitoring period and clipped them to the region of interest using

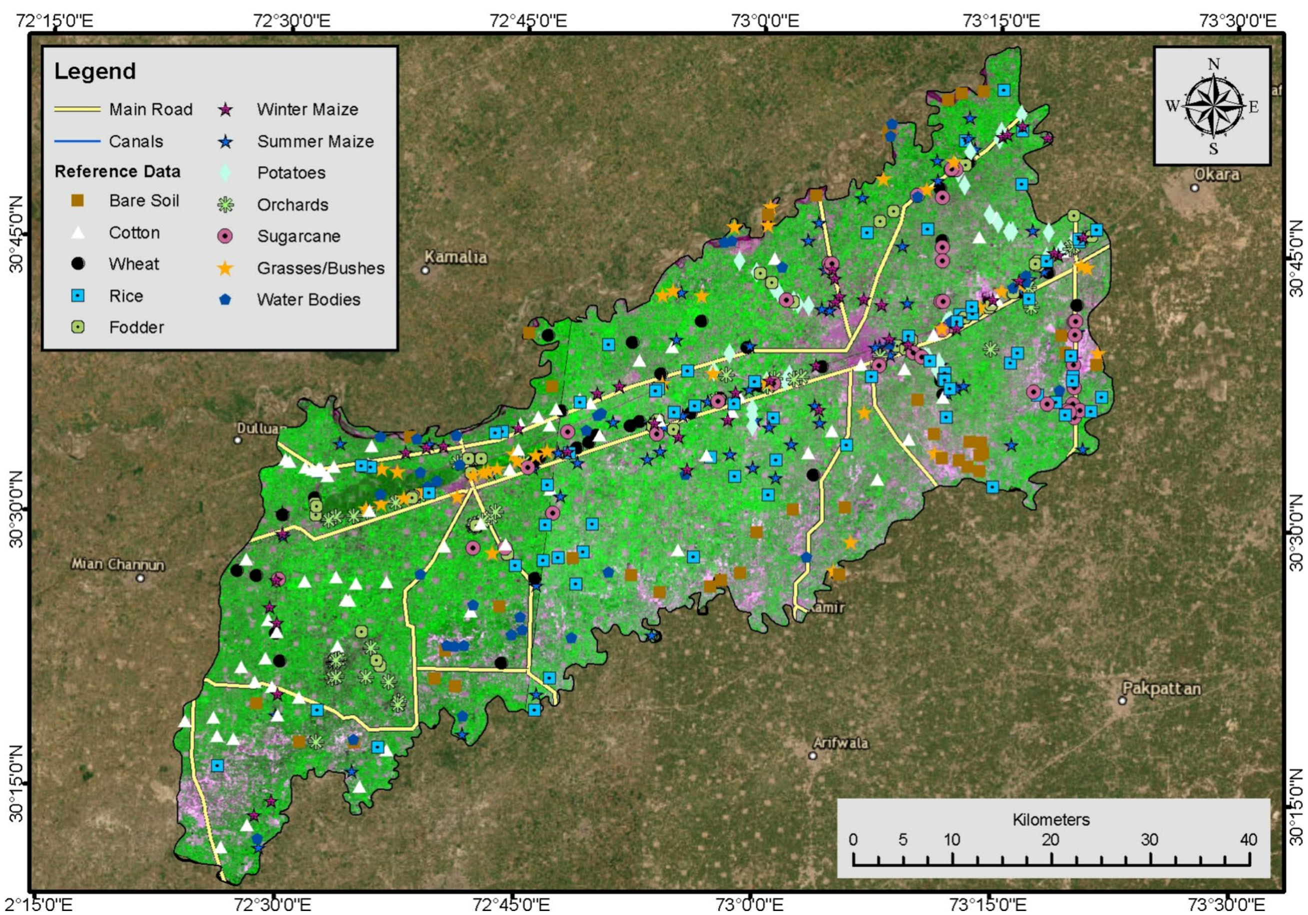

Fig. 3 Map of in situ data collected for the research

Fig. 4 Research flow diagram

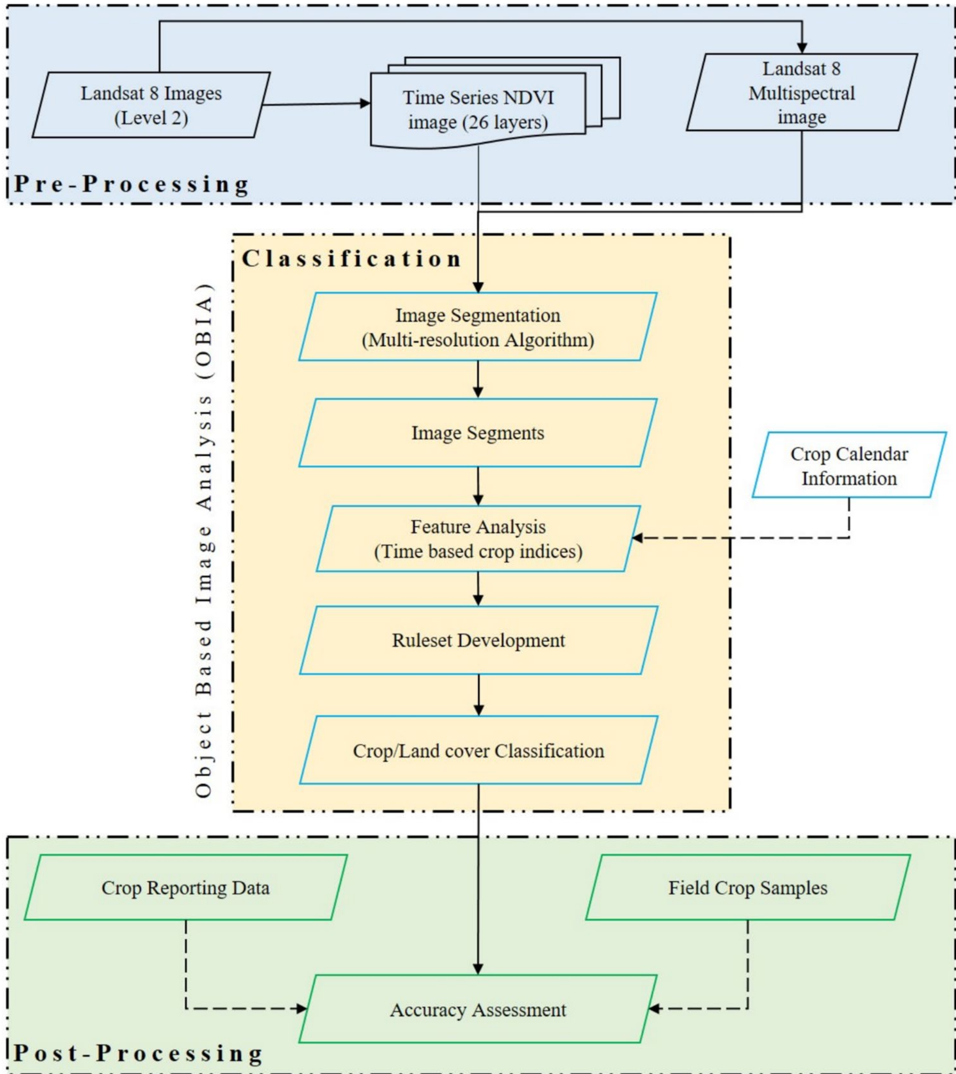

ERDAS IMAGINE 2014. These selected images were used to extract *NDVI* values and organize them into two stacked and time series *NDVI* datasets for the Rabi and Kharif cropping seasons. The multispectral image of Landsat 8 was also processed to be used along with temporal *NDVI* stacks in OBIA to distinguish non-vegetative land cover features, such as water bodies, bare soil etc.

2.3.2 Preparation of Temporal Profiles of NDVI

NDVI is a well-known index that utilizes chlorophyll's absorptive and reflective properties to distinguish vegetation from other land cover features [30]. *NDVI* employs Red (band 4) and Near Infrared (band 5) bands (ρ) of a satellite image (Landsat 8 in this case) to enhance vegetation using the following formula (Eq. (1)) [34]:

$$\mathrm{NDVI} = \frac{\rho_{(NIR)} - \rho_{(red)}}{\rho_{(NIR)} + \rho_{(red)}} \tag{1}$$

All *NDVI* layers extracted from 23 Landsat 8 images, i.e., 11 images for the Rabi and 12 images for the Kharif season (as described in Table 1) were stacked to obtain temporal phenological information for the study area. Low-pass filters were also applied to the temporal *NDVI* layers to remove noise and obtain a smooth *NDVI* pattern for each crop. The comparison of raw and filtered *NDVI* images for samples of wheat and rice (A), and potatoes and maize (B) is demonstrated in Fig. 5.

Table 1 Dates of satellite images used, cropping season, and field samples

No	Date	Day of year (DoY)	Cropping season	Field survey	Collected samples
1	12-Oct-20	285	Rabi		
2	28-Oct-20	301	Rabi		
3	13-Nov-20	317	Rabi		
4	29-Nov-20	333	Rabi		
5	15-Dec-20	349	Rabi		
6	31-Dec-20	365	Rabi		
7	16-Jan-21	16	Rabi		
8	17-Feb-21	48	Rabi	Yes	Wheat, potatoes, sugarcane, Kharif maize, orchards, fodder, grasses/bushes, bare soil, water bodies
9	05-Mar-21	64	Rabi	Yes	
10	21-Mar-21	80	Rabi	Yes	
11	06-Apr-21	96	Rabi		
12	22-Apr-21	112	Kharif		
13	08-May-21	128	Kharif		
14	24-May-21	144	Kharif		
15	09-Jun-21	160	Kharif		
16	25-Jun-21	176	Kharif		
17	11-Jul-21	192	Kharif		
18	27-Jul-21	208	Kharif		
19	12-Aug-21	224	Kharif	Yes	Rice, cotton, sugarcane, Rabi maize, orchards, grasses/bushes, bare soil, and water bodies
20	28-Aug-21	240	Kharif	Yes	
21	13-Sep-21	256	Kharif	Yes	
22	29-Sep-21	272	Kharif	Yes	
23	15-Oct-21	288	Kharif		

2.3.3 Classification Through OBIA

The prepared *NDVI* stack images were imported into eCognition 8 along with a single multispectral image for object-based image analysis (OBIA). The prepared dataset was used to create crop indices from cropping calendar information to develop a rule set for crop classification.

Segmentation Segmenting is the primary step for satellite image classification through OBIA, in which image pixels are converted into objects/segments with more or less similar spectral and physical characteristics [2]. First, *NDVI* time series of 23 layers along with two multispectral images for Rabi and Kharif were imported into eCognition 8 for crop and land cover mapping through a rule set-based algorithm. In this research, multispectral images were also used in OBIA to distinguish other land cover features, such as water and soil. Once the non-cropping land cover classes were separated, all the threshold ranges were defined to distinguish one crop from another using a crop index based on *NDVI* time series. Segmentation is a repetitive process of achieving the most suitable segments/objects by trial-and-error method. This process is controlled by choosing the appropriate parameters values for scale, compactness, and shape [37]. As the primary objective of this research is to develop a semi-automatic algorithm for crop classification using crop indices, we chose the scale (5), where we obtained the segments with minimum pixels. In this way, more homogeneous or pure segments were not only obtained, but the possibility of errors due to segmentation was also minimized.

Feature Analysis and Crop Index Development Crop indices for individual crops were developed by adopting the same approach used in various well-known spectral indices, such as *NDVI* [34], enhanced vegetation index (*EVI*) [39], normalized difference water index (*NDWI*) [6], modified normalized difference water index (*MNDWI*) [46], and others. The primary principle of these indices is to utilize two spectral bands with maximum and minimum reflectance characteristics for a particular land cover feature and use their reflectance difference to enhance or distinguish one feature from another. Similarly, two time-based *NDVI* were used to develop a crop index to distinguish a particular crop from others. One of the two *NDVI* corresponds to the time when the crop is in its mature cropping stage, where it has the maximum *NDVI* value. In contrast, the other *NDVI* corresponds to the time when the crop is in its initial stage and has a lower or minimum *NDVI* value. Thus, this approach can be expressed as an equation (Eq. (2)):

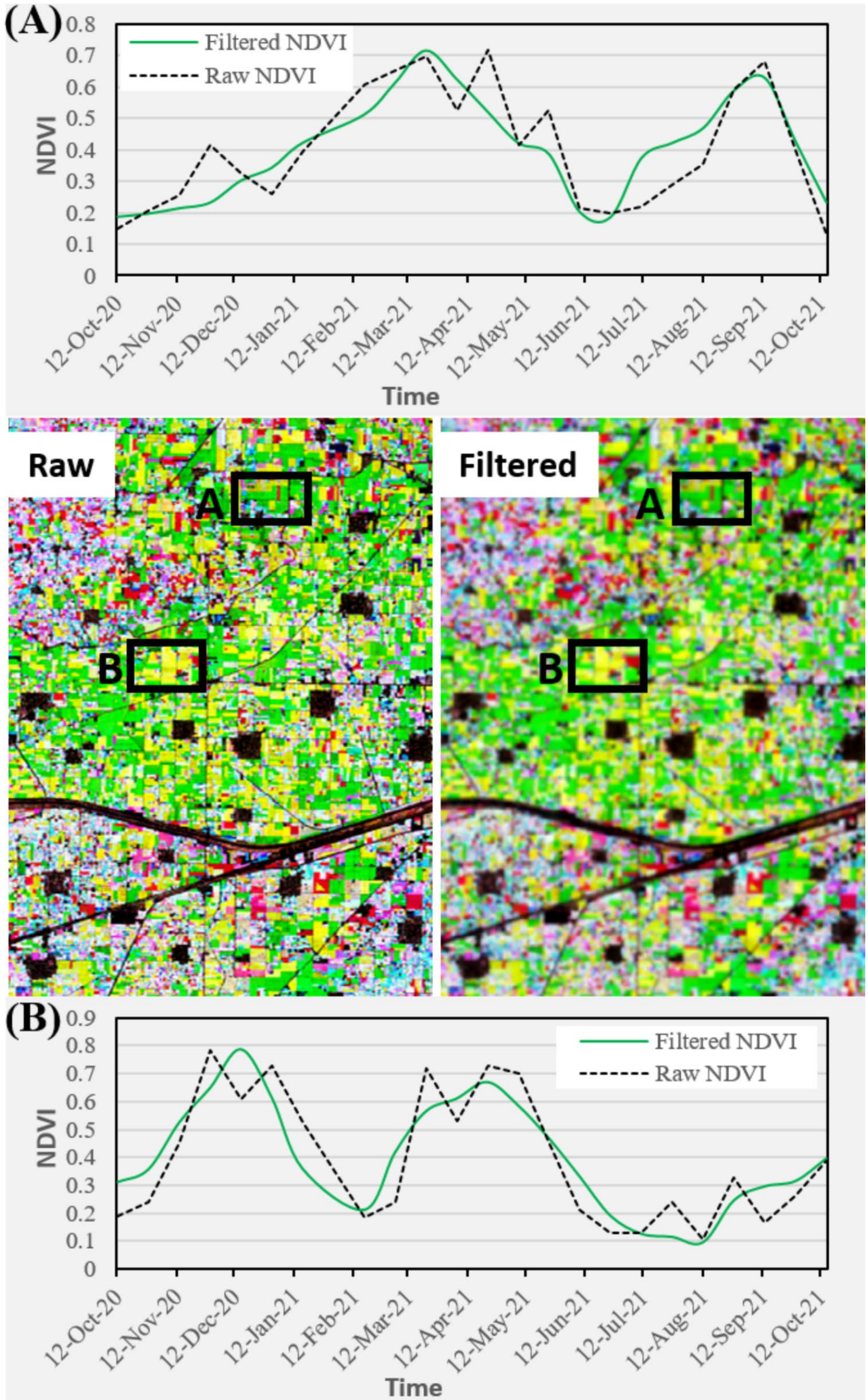

Fig. 5 Raw and filtered *NDVI* stack and pattern. **A** Wheat and rice; **B** potatoes and maize

$$Cropindex = \frac{NDVI_{(m)} - NDVI_{(i)}}{NDVI_{(m)} + NDVI_{(i)}} \tag{2}$$

where *NDVI*(*m*) and *NDVI*(*i*) are the values of *NDVI* at the mature and initial or harvested cropping stages, respectively. For example, wheat is planted in Sahiwal district, spanning from mid-October to the end of November, and its phenological information at this initial stage can be detected in satellite images, although the captured reflectance is weak due to sparseness and soil exposure. Similarly, when wheat reaches its mature or development stage during March and April, it exhibits maximum reflectance (high *NDVI* value) due to vigorous chlorophyll content in its relatively dense canopy [14]. In the subsequent harvesting stage, from mid-April to the start of May, the crop begins to senescence, dry out and lose its greenness causing chlorophyll levels to reduce, resulting in lower *NDVI* values. The phenological information is transformed into a crop index to distinguish wheat from other crops using the crop index as described in above equation (Eq. (2)). The index for wheat in day of the year (DOY) format can be written as (Eq. (3)):

$$Wheatindex = \frac{NDVI_{(64)} - NDVI_{(333)}}{NDVI_{(64)} + NDVI_{(333)}} \tag{3}$$

$NDVI_{(64)}$ and $NDVI_{(333)}$ are the *NDVI* values extracted from Landsat images on DOY 64 and 333, dated 5 March 2021 and 29 November 2020, respectively, as seen in Table 1. Crop indices for remaining crops are also developed (Eqs. (5), (6), (7,) and (8)) based on their crop stage information, using crop calendar mentioned in Fig. 2.

$$Summermaizeindex = \frac{NDVI_{(112)} - NDVI_{(48)}}{NDVI_{(112)} + NDVI_{(48)}} \tag{4}$$

$$Potatoindex = \frac{NDVI_{(334)} - NDVI_{(48)}}{NDVI_{(334)} + NDVI_{(48)}} \tag{5}$$

$$Cottonindex = \frac{NDVI_{(208)} - NDVI_{(256)}}{NDVI_{(208)} + NDVI_{(256)}} \tag{6}$$

$$Riceindex = \frac{NDVI_{(240)} - NDVI_{(176)}}{NDVI_{(240)} + NDVI_{(176)}} \tag{7}$$

$$Wintermaizeindex = \frac{NDVI_{(256)} - NDVI_{(176)}}{NDVI_{(256)} + NDVI_{(176)}} \tag{8}$$

Rule Set Development The rule set is the hierarchy of processes in OBIA consisting of segmentation, defining ranges for different land cover classes using satellite images, indices, and thematic data [33]. In this research, we used a hierarchical approach to distinguish one land cover class or crop type from another. One of the advantages of using OBIA-based hierarchical classification approach is the ability to apply threshold conditions to the segments of a particular class and leave the remaining segments intact. This is not the case in conventional pixel-based classification, in which any applied modification affects all pixels each time [3].

In this research, the combination of multispectral and time series *NDVI* from Landsat 8 provided the spectral and phenological patterns of land cover features. A top-down

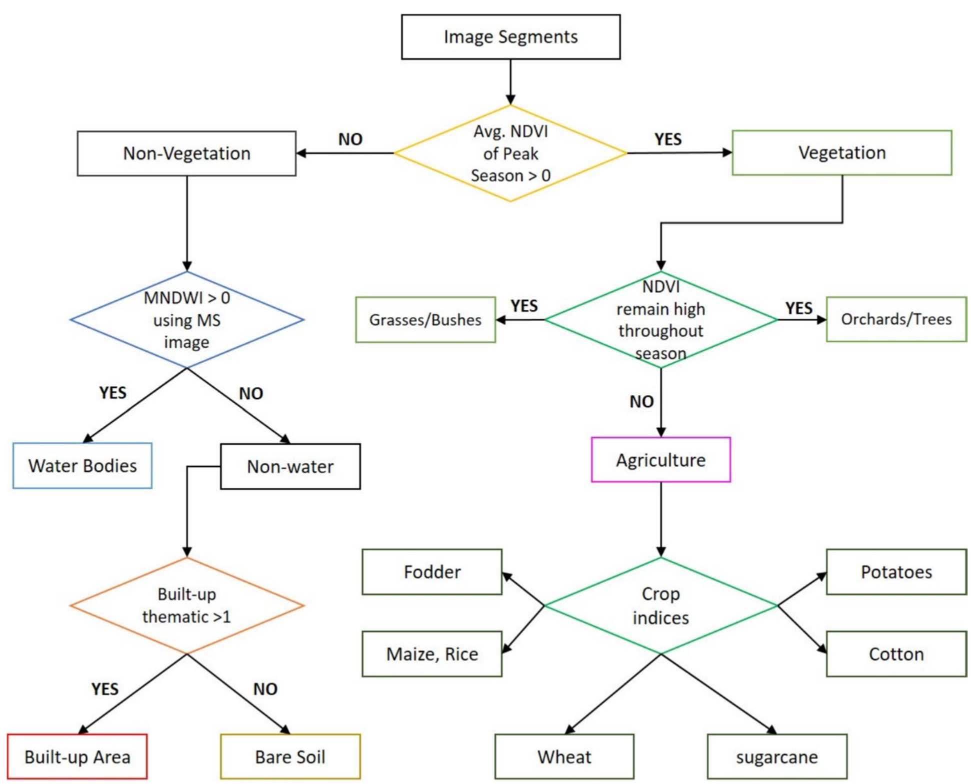

Fig. 6 Rule set developed in the research for crop classification

hierarchical OBIA approach (as shown in Fig. 6) was adopted, as it enhances classification accuracy and efficiency by considering contextual information at multiple scales, starting with larger datasets or objects and progressively refining them into smaller, more specific objects using expert knowledge [42]. For example, first, broad land cover classes, namely vegetation and non-vegetation, were identified using the average *NDVI* of the peak cropping stage and then divided into their sub-classes using the mean values spectral and phenological patterns. The classification was carried out for both cropping seasons (i.e., Rabi and Kharif) separately, using crop calendar information. Furthermore, as trees/orchards and grasses/bushes exhibit a notable *NDVI* value throughout the year with few seasonal changes, this pattern was utilized to distinguish these classes from the rest of the vegetation class, i.e., agriculture. The agriculture class was further divided into individual crops using their indices using Eqs. (3), (4), (5), (6), (7), and (8). The entire rule set developed for this research using OBIA can be seen in Fig. 6. In addition, the *MNDWI* was also employed to separate water bodies from the non-vegetation classes. The rest of the non-vegetation class was further divided into the built-up areas and bare soil using pre-developed vector data of settlements as a thematic layer in OBIA. The entire classification process was performed in Trimble's eCognition image processing software.

2.4 Accuracy Assessment

Finally, the accuracy of the crop classification results was assessed in two ways. First, field validation samples were used for the accuracy assessment of each crop. To ensure the accuracy of the delineated boundaries of segments, we adopted a specific field survey approach. Each crop sample was delineated by recording the coordinates at the four corners of the crop field using a GPS device. These coordinates were then used to create polygonal boundaries by joining these corner points, accurately delineating the crop field. This method ensured that the segment boundaries accurately represented the actual field boundaries, thereby enhancing the quality of the segments and, consequently, the final classification results. A confusion matrix was developed to compare crop classification with field samples for each crop. Subsequently, the kappa coefficient was also calculated, along with the user's, producer's, and overall accuracy values, to assess the classification results. Additionally, the area of each crop was also compared with the crop reporting service (agriculture department) data to measure the agreement between estimated results and crop area statistics. This comparison was described in the form of a percentage difference.

3 Results

The key components and results of the research methodology are illustrated in Fig. 7. This figure summarizes the multiple steps as followed in the research methodology, each step contributing to a comprehensive understanding of crop and land cover dynamics. At the core of this analysis is the Landsat 8 multispectral image (Fig. 7A), acting as the foundational layer upon which subsequent results were developed. The contrasting interplay of brighter and darker pixels facilitates a visual demarcation of these vital distinctions, respectively.

The mean temporal *NDVI* pattern for the crops in the test sites of the study area is shown in Fig. 8. All the crops showed a unique phonological cycle with peaks associated with their mature growing stages. The *NDVI* profile of Rabi crops (Fig. 8A) showed that the peak value of the wheat crop was obtained around mid-February, while the harvest date was in late April, which was also cross-validated with the crop calendar (Fig. 2) of the study area. Similarly, the other two main crops of the Rabi season showed their peak and minimum *NDVI* values associated with their growing and harvesting periods, respectively. The same applies to the main crops of the Kharif season (Fig. 8B). The unique phenological patterns of each crop were used in the preparation of the crop index for each respective crop using Eq. (1). All the annual crops, i.e., sugarcane, fodder, and orchards, show haphazard and random *NDVI* profiles due to their phenological cycles, as seen in Fig. 8 C, and are therefore identified using their composite spectral and phenological characteristics.

All the crop indices were developed by selecting two *NDVI* layers at the appropriate times, as mentioned in the crop index (Eq. (1)). As the crop starts to germinate and establish itself, the initial *NDVI* values captured by satellite sensors may be relatively low due to greater contribution from soil reflectance. Similarly, at the harvesting stage, the *NDVI* values were also observed to be low due to the drying out of chlorophyll or greenness. In contrast, at the mature or development stage, the crop exhibits maximum *NDVI* values due to high chlorophyll content. Therefore, the "*NDVI* Min" and "*NDVI* Max" layers for a particular crop index, as mentioned in Table 2, are associated with $NDVI_i$ and $NDVI_m$ of Eq. (1). The selected *NDVI* layers used in developing the crop indices for each crop are summarized in Table 2.

Furthermore, sugarcane and fodder are annual crops that exhibit distinct growth and reflectance patterns because they are frequently harvested by the local community based on their specific requirements. This dynamic cycle of harvest, regrowth, and is influenced by local practices, resulting in *NDVI* fluctuations that are not solely

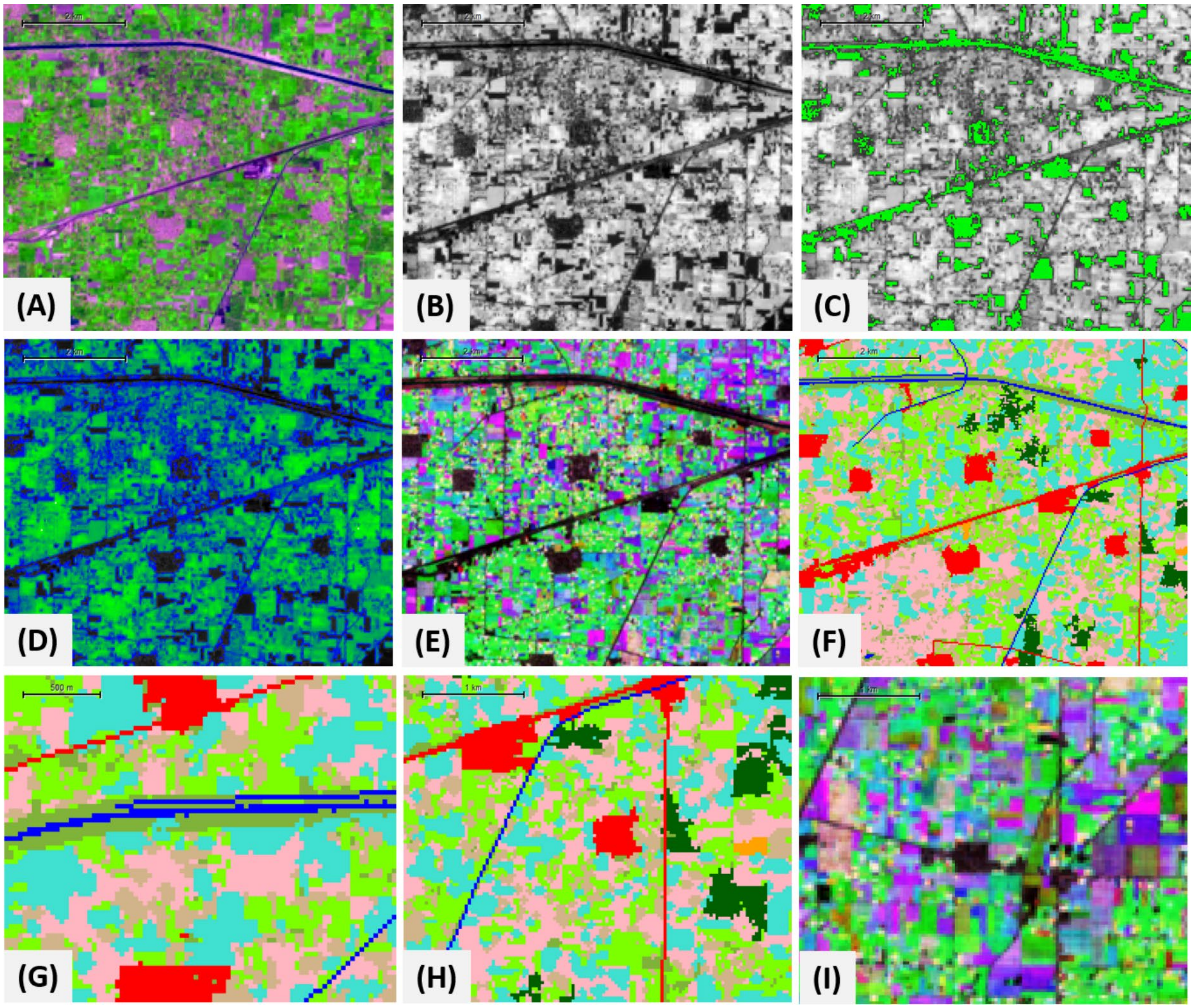

Fig. 7 Insets of key components of research methodology **A** Landsat 8 multispectral image of Rabi season dated 13-Sep-2021; **B** *NDVI* layer brighter pixels represent vegetative land, while non-vegetative is depicted by dark pixels; **C** selected pixels of non-vegetative land with $NDVI < 0$ in the green shade; **D** vegetative pixels with $NDVI > 0$; **E** stack of *NDVI* layers with band combination RGB: 22 Nov 2020, 20 Feb 2021, and 15 April 2021; **F** presents a detailed crop classification map; **G** portrays grasses and bushes along a water channel in a subtle green hue, complemented by blue for the water; **H** showcase of distinct patches of orchards/trees in a dark green shade; **I** vividly displays agricultural patches with various crops depicted in multiple colors, with darker tones indicating non-vegetative land or settlements

indicative of the crop's true phenological cycle. Given this unique characteristic, these annual crops remain less concentrated in order to provide a more accurate and representative depiction of the other crop indices.

In Fig. 9, all the eight crop indices are compared visually at a subset of the study area. The dominant crop in the selected subset is maize in the Rabi season, followed by potatoes and Kharif maize. In this figure, a higher value (represented by blue tones) indicates a higher likelihood of the presence of the crop whose index is under observation, and vice versa. For example, in the maize index (Fig. 9), blue pixels represent the highest likelihood of the presence of maize crop, which is the dominant crop in the selected subset, while red pixels indicate the lowest likelihood of its presence. Furthermore, potatoes and Rabi maize, which are major crops, usually replace Kharif maize, show the maximum values in their respective indices. This was also verified through observation. The point to be noted is that the area of potatoes and Kharif maize are almost identical because potatoes, a 3-month crop, are typically replaced by Kharif maize, as verified by farmers during the field survey. In contrast, due to the minimal presence of wheat, cotton, and rice crops in the selected subset, the indices of these crops showed minimum values.

Crop maps, using crop indices with semi-automatic OBIA, are produced for the two cropping seasons, i.e., Rabi 2020–2021 and Kharif 2021, as shown in Fig. 10. The spatial distribution of crops in the maps showed that most of the land in the study area is agricultural (Table 3) and exhibits a double cropping pattern due to intense irrigation

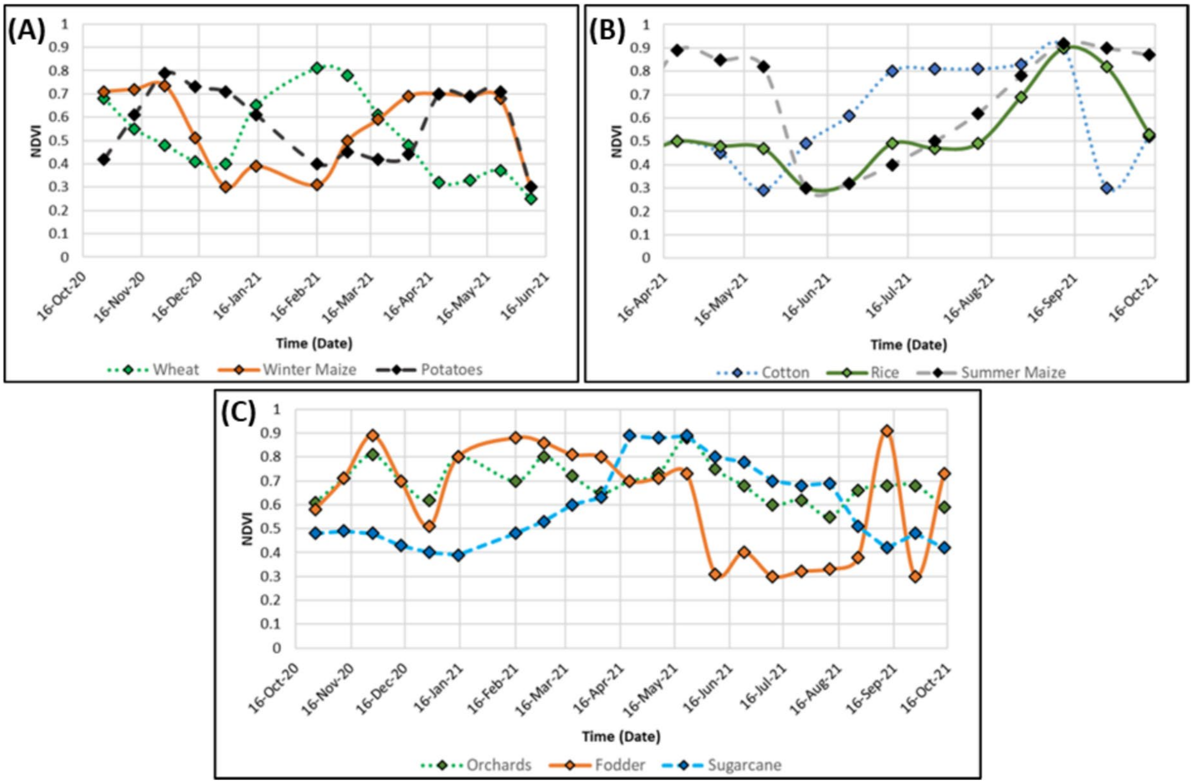

Fig. 8 Time-based *NDVI* profiles of Rabi (**A**), Kharif (**B**), and (**C**) annual crops

Table 2 Selected *NDVI* used in crop indices of each crop

Crop index	*NDVI*·Max	*NDVI*·Min	Band no. in stack
Wheat	05-Mar-21	31-Dec-20	9.6
Kharif maize	22-Apr-21	17-Feb-21	12.8
Potatoes	29-Nov-20	17-Feb-21	4.8
Cotton	27-Jul-21	13-Sep-21	18.21
Rice	28-Aug-21	25-Jun-21	20.16
Rabi maize	13-Sep-21	25-Jun-21	18.16

infrastructure. It was also confirmed from the maps that wheat (43.8%) is the most dominant crop in the Rabi season, while cotton (19.5%) along with Kharif maize (30.7%) are the major crops in the Kahrif season. The crop maps also showed inconsistent cultivated field sizes across the region, aligned with local farmers' need and the cultivatable area they own.

3.1 Accuracy Assessment

The accuracy assessment of crop maps, for both cropping seasons, exhibits a fairly high precision, summarized in Tables 4 and 5, respectively. The accuracy assessment of a classified map involves the comparison of the number of points classified by the classification algorithm, also known as the "classified total" with the actual land cover class or the "reference total". This comparison is used to estimate overall accuracy (number of corrected classified pixels/total number of pixels), producer's accuracy (number of corrected classified pixels/number of reference pixels for the class), user's accuracy (number of corrected classified pixels/number of classified pixels for the class), confusion matrix, and kappa coefficient (Tables 4 and 5) [11]. Overall classification accuracy for Rabi crops was observed at 84.7%, and 86.1% for summer crops, with kappa coefficient values of 0.83 and 0.84, respectively (Tables 4 and 5). The wheat crop was observed as the most accurately estimated crop in the Rabi cropping season, with 88% user and 85% producer accuracies. Maize, orchards, and sugarcane in the Rabi season had the average accuracy of approximately 85%. Wheat, along with maize, orchards, and sugarcane, covered about 74% of cultivable land in the Rabi cropping season, indicating that 74% of cultivable land in our study area was estimated with 85% of accuracy. The producer and user accuracy for potatoes and fodder were observed to be relatively low (less than 80%) due to two possible reasons. First, although the fodder crop covered approximately 15% of the cultivable area during the Rabi season, the average field size of fodder is much smaller than the pixel size of the Landsat image (30 × 30 m). This is because fodder is not a commercial crop, and farmers cultivate it for their household needs. Fodder

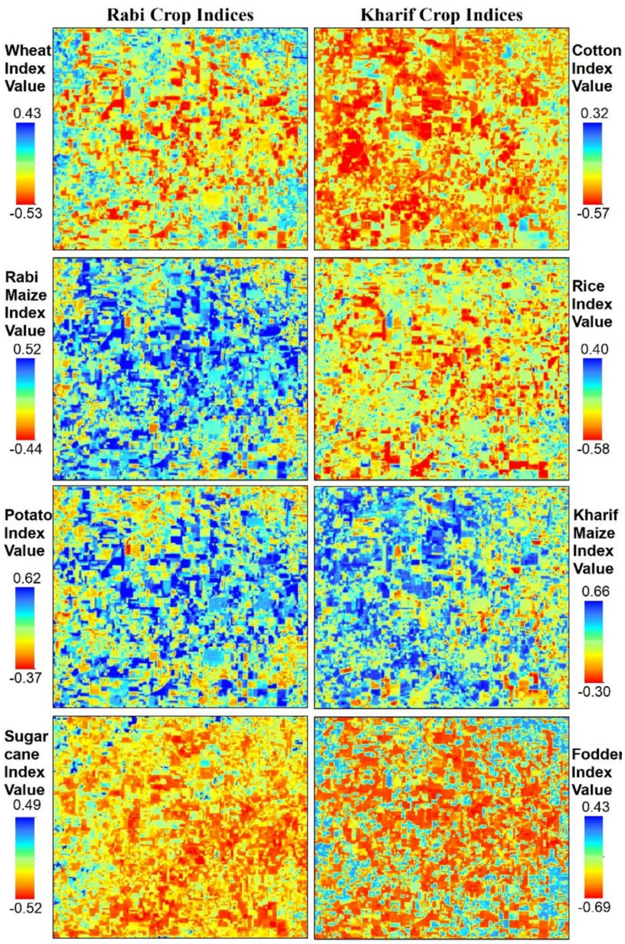

Fig. 9 Six crop indices of the same subset in the study area

is also not a 6-month crop, instead, some farmers sow it twice during one cropping season based on their household needs, resulting in lower observed accuracy due to its multiple and diverse phenological cycles. Furthermore, the lower observed accuracy for fodder aligns with challenges noted in previous studies, where small field sizes and variable phenological patterns complicate classification, particularly using moderate resolution satellite imagery, like Landsat (30 m). For instance, Singha et al. [37] reported similar difficulties in classifying fragmented paddy fields in Northeast India, attributing lower accuracies to mixed pixels and irregular cropping patterns. The same issue was also highlighted by Löw and Duveiller [25] for crop identification in Central Asia, suggesting that moderate resolution imagery is sufficient for major crops but less suitable for heterogeneity cropping pattern and small field sizes. In our case, fodder fields, often smaller than 30 m × 30 m, likely result in mixed pixels, lowering classification accuracy. Belgiu and Csillik [2] suggested that higher-resolution imagery (e.g., Sentinel-2 at 10 m) or denser temporal data could improve accuracy for such crops. Second, potatoes are also a 3-month crop, typically followed mainly by summer maize or fodder, so their phenological cycle was also mixed with other crops during the early summer season due to the relatively low temporal resolution of Landsat (16 days).

The results of the accuracy assessment for summer crops are summarized in Table 5. Overall classification accuracy for summer crops was observed at approximately 86%, with a kappa coefficient value of 0.84. The cultivable land for cotton, summer maize, orchards, and sugarcane crops was estimated with an overall accuracy greater than 87%. These crops covered approximately 70% of the cultivable area in the summer season. The rice crop grows in two cropping phases, namely rice paddies and the main; consequently, due to abrupt changes in its phenological cycle from these two distinct cropping phases, the accuracy of rice was observed to be relatively low (~ 78%), compared to other crops. Fodder again has relatively low accuracy in the summer season due to the same reasons, as mentioned above. It was also noted that non-cropping land cover classes also had fairly high accuracies when classified using composite data from phenological and multispectral information through a hierarchical classification approach.

The estimated crop area for each crop in both cropping season was also compared with statistics published by the crop reporting service (CRS) of the Agriculture department. The CRS is responsible for reporting the district-wise area across the entire province through extensive field surveys conducted by thousands of its field staff. The comparison of the total crop area of Rabi (Fig. 11a) and Kharif (Fig. 11b) crops in the study area during 2021–2021 suggested that the most dominant crops, i.e., wheat, cotton, Rabi, and summer maize, were estimated with the accuracies of approximately 91%, 88%, 93%, and 92%, respectively. The rest of the crops were also estimated with more than 90% accuracy (Fig. 11) except for fodder, which was estimated with more than 80% accuracy. This means, most of the agricultural land during both cropping seasons was identified with fairly high precision using the methodology adopted in this study. Therefore, this approach is a good alternative for efficiently estimating different crop areas, avoiding extensive field surveys that consume excessive resources and time.

4 Discussion

Distinguishing crops from other vegetation types using a single multispectral image is not a simple task [21]. However, satellite images acquired at different stages of crop growth play an important role not only in discriminating crops from other vegetation types but also in separating one crop from another [29]. These images also effectively improve the overall accuracy of crop classification when used properly with the knowledge of the local crop calendar and phenological

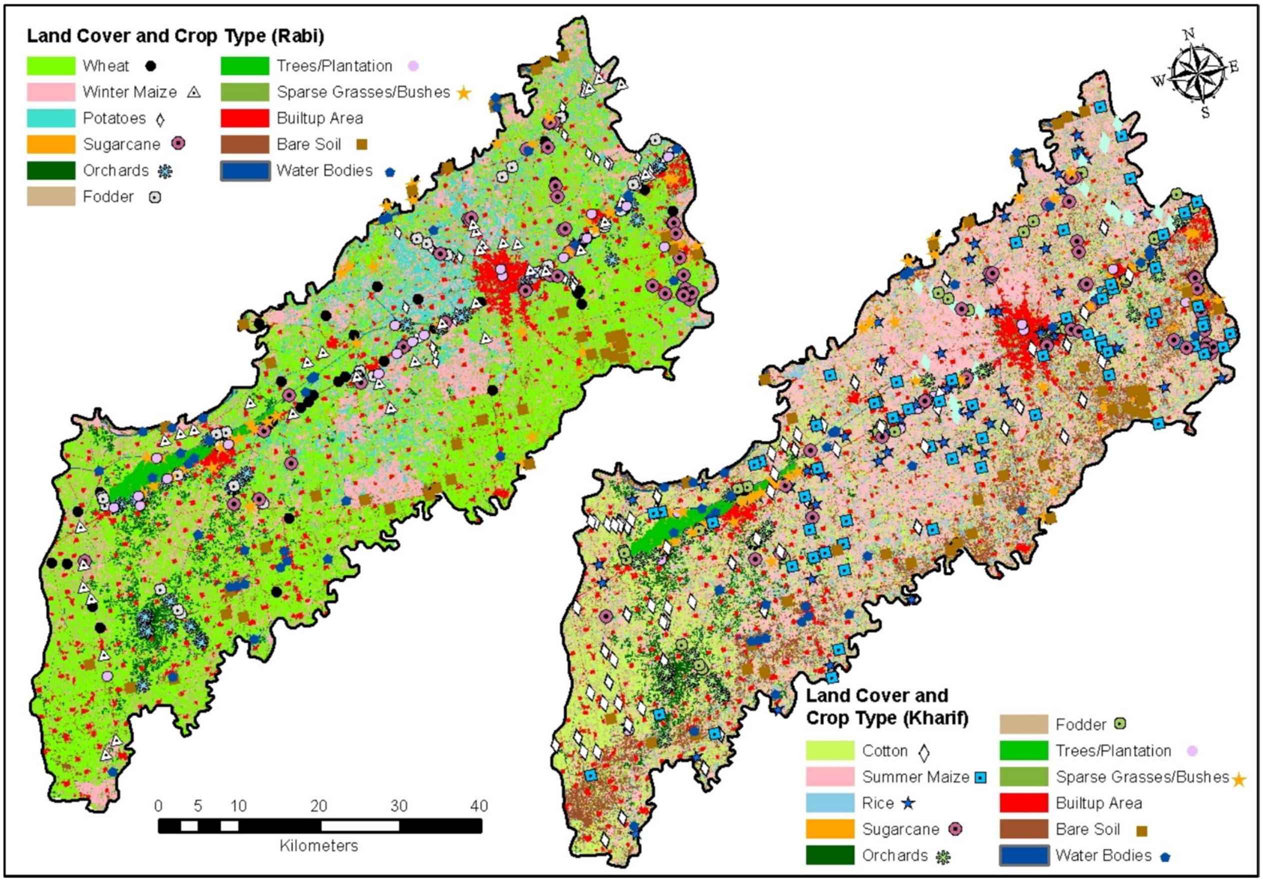

Fig. 10 Land cover and crop type maps of Rabi and Kharif seasons with reference data for the cropping year 2020–2021

Table 3 Land and crop cover area as estimated in the research for Rabi (2020–2021) and Kahrif (2021)

	Rabi season			**Kharif season**		
	Class name	**LC area (km^{2})**	**(%)**	**Class name**	**LC area (km^{2})**	**(%)**
1	Wheat	1405.75	43.84	Cotton	624.69	19.48
2	Maize	462.84	14.43	Rice	285.57	8.91
3	Potatoes	279.81	8.73	Maize	983.82	30.68
4	Orchards	105.10	3.28	Orchards	105.08	3.28
5	Fodder	418.45	13.05	Fodder	462.04	14.41
6	Sugarcane	45.91	1.43	Sugarcane	50.36	1.57
7	Trees/plantation	52.04	1.62	Trees/Plantation	54.09	1.69
8	Grasses/bushes	131.06	4.09	Grasses/Bushes	81.64	2.55
9	Built-up area	235.06	7.33	Built-up Area	235.05	7.33
10	Bare soil	42.72	1.33	Bare Soil	296.33	9.24
11	Water bodies	27.79	0.87	Water Bodies	27.94	0.87

details [31, 43]. In our study area, vegetation types are very diverse, irregular, and spatially fragmented along with other non-vegetative features. Distinguishing major vegetation types from one another using remotely sensed phenological information is quite a challenging task due to variable crop planting times, patterns, small field sizes, local weather conditions, diversity, and other factors. Therefore, a hierarchical approach has been devised for such a heterogeneous study area. This could not be achieved easily through conventional pixel-based classification techniques, which incorporate spectral values only and operate on the entire image simultaneously [38]. Therefore, an object-based

Table 4 Accuracy assessment crop classification for Rabi cropping season

Class name	Reference totals	Classified totals	Corrected	Producer accuracy	User accuracy
Wheat	26	25	22	85%	88%
Maize	24	25	20	83%	80%
Potatoes	25	25	19	76%	76%
Orchards	24	25	21	88%	84%
Fodder	31	25	19	61%	76%
Sugarcane	23	25	21	91%	84%
Trees/plantation	22	25	20	91%	80%
Sparse grasses/bushes	26	25	19	73%	76%
Built-up Area	25	25	24	96%	96%
Bare soil	24	25	23	96%	92%
Water bodies	25	25	25	100%	100%

Overall classification accuracy = 84.73% and overall kappa statistics = 0.83

Table 5 Accuracy assessment crop classification for Kharif cropping season

Class name	Reference totals	Classified totals	Corrected	Producer accuracy	User accuracy
Cotton	26	25	21	83%	86%
Rice	24	25	19	79%	76%
Maize	23	25	21	91%	84%
Orchards	25	25	22	88%	88%
Fodder	30	25	19	63%	76%
Sugarcane	22	25	22	100%	88%
Trees/plantation	25	25	21	84%	84%
Sparse grasses/bushes	26	25	22	85%	88%
Built-up area	26	25	24	92%	96%
Bare soil	26	25	23	88%	92%
Water bodies	22	25	22	100%	88%

Overall classification accuracy = 86.18% and overall kappa statistics = 0.84

image analysis (OBIA) approach was adopted to meet the objective of the research.

The choice of OBIA over traditional pixel-wise classification, including machine learning approaches, was driven by the need to integrate phenological and contextual information effectively in a heterogeneous agricultural landscape. Pixel-wise methods, which rely solely on spectral values, often struggle to distinguish crops with overlapping spectral signatures, especially in regions with small, irregular fields and variable sowing times, as observed in Sahiwal. In contrast, OBIA uses the object-level spectral, temporal, and spatial features, enabling more accurate delineation of crop types based on phenology. This advantage is well-documented in similar studies. For example, Duro et al. [10] demonstrated that OBIA outperforms pixel-wise machine learning classifiers (e.g., Random forest and SVM) in capturing phenological dynamics across fragmented croplands, even with fewer variables, in Alberta, Canada. Similarly, Zhang et al. [49] applied OBIA with multi-temporal SPOT-5 imagery (10 m resolution) and a Random forest classifier to classify crops in a heterogeneous landscape, extracting spectral reflectance, vegetation indices, and textural features (e.g., geo-statistical semivariogram). They highlighted OBIA's ability to integrate diverse data types and ML algorithms beyond spectral values, a flexibility unattainable in pixel-wise ML methods like support vector machines or standalone RF, which typically process pixels independently without spatial context. Modern RF applications further evolve the classification techniques, for example Mahmood et al. [27] used RF with 122 SAR and optical features from Sentinel-1 and Sentinel-2 time series in Punjab, Pakistan, demonstrating that RF can now incorporate multiple suitable features (e.g., VH SAR data during cloud cover) for crop classification. Their feature reduction retained 98% accuracy after omitting 80% of features, highlighting RF's robustness with multi-source data. However, this pixel-wise approach lacks the object-level contextual analysis that OBIA provides, which is crucial for delineating small, variable fields

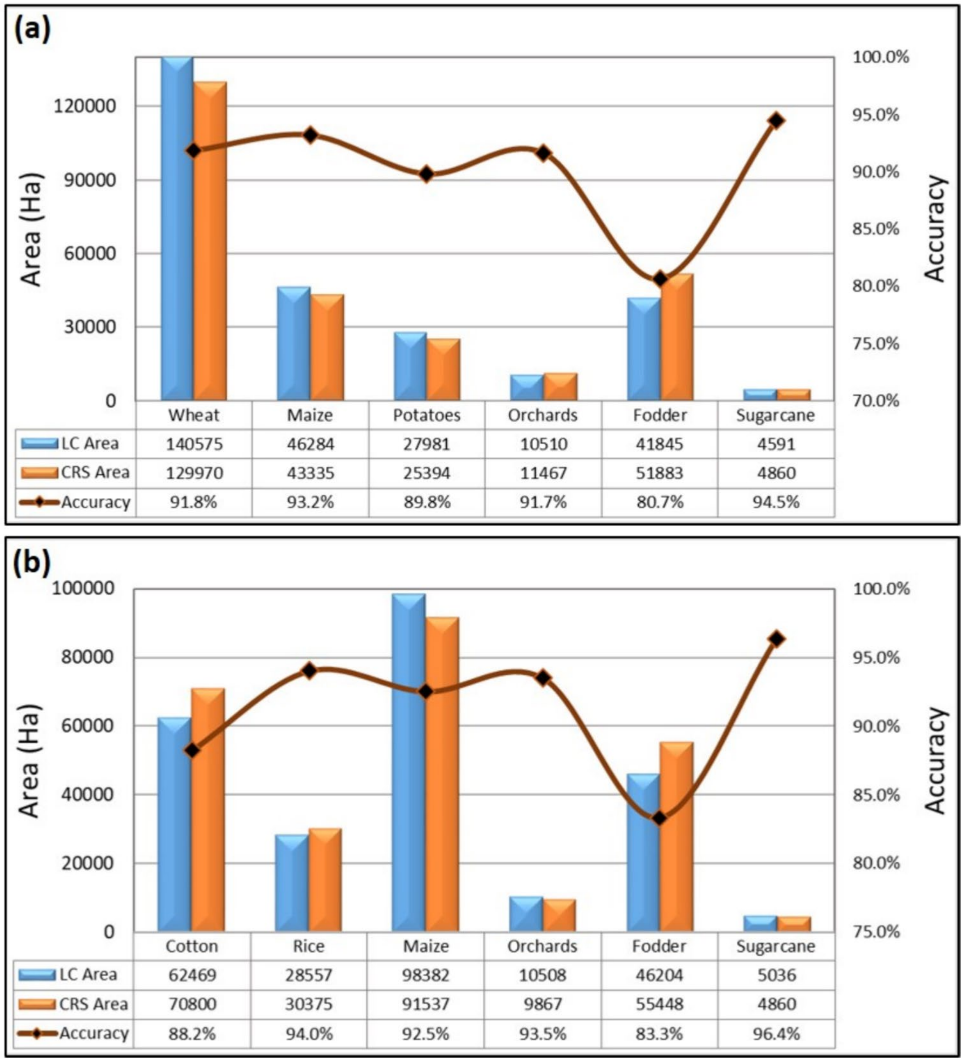

Fig. 11 Comparison of the estimated crop from developed Landover (LC) and observed crop area from Crop Reporting Service (CRS)—Agriculture Department; **a** Rabi cropping season; b summer cropping season

in Sahiwal. Our OBIA method, using hierarchical top-down classification, first separated general land cover classes (e.g., vegetation vs. non-vegetation) with multispectral and *NDVI* data and then refined crop-specific indices. Unlike pixel-wise methods, which reprocess the entire image with each adjustment, OBIA allowed us to apply threshold conditions to specific segments without affecting others, enhancing efficiency and accuracy.

In the current study, image classification was executed using a single-time multispectral image combined with temporal phenological information. Crop classification using multispectral data only can lead to misclassification due to the shared spectral characteristics of crops and other vegetative features, e.g., grassland, natural vegetation, and forest [48]. On the other hand, a combination of spectral and phenological data significantly enhances the crop classification results [37]. The main reason behind the use of composite data of spectral and phenological cycles is that different crops and other vegetation types often exhibits similar spectral characteristics [50]. Therefore, by capturing the phenology at different growth stages, one crop can be separated from the other crops and vegetation types more efficiently [17]. This study verified the effectiveness of using a combination of spectral and phenological information for cropland mapping through an object-based image classifier in a hierarchical (top-down) manner. Considering previous study conducted by Zhong et al. [51] and Peña et al. [32], the current study makes a distinct and important contribution to the relevant field, as we focused on developing a simple, efficient, and robust approach to crop classification. This study demonstrated how phenological information from temporal data at the initial and peak growing stages of different crops can be utilized for accurate cropland classification. Additionally, using phenology at different growth stages, rather than the entire cycle, allows the use of alternate consecutive temporal images when data missing due to cloud cover.

In this research, minimum possible phenological data (at major growth stages) from Landsat imagery was used along with local crop calendar information to develop crop indices for each crop to distinguish them from one another. The selected images from specific time period during important crop growth stages have the potential to discriminate multiple crops based on variations in their phenology cycles [41]. Chakhar et al. [5] assessed in a recently published review article that even the combined use of Landsat and Sentinel-2 A spectral imagery did not significantly enhance the results of crop classification. In this research, spectral images were also used in a hierarchical (top-down) classification approach to differentiate general land cover classes (e.g., soil, natural vegetation, built-up areas, and water bodies). These classes were separated by adjusting and applying appropriate threshold conditions for each class without affecting the segments of other classes. Thus, the adopted top-down hierarchical method logically separated non-cropping classes at the initial stages of classification, making the subsequent process easier and more efficient without affecting previously classified features.

In the previous studies by Hao et al. [15] and Murakami et al. [28], it was shown that, rather than processing the entire growing season of a crop, images from some optimal growth stages can provide high accuracy for cropland mapping. Furthermore, Wardlow et al. [44] suggested that, when performing crop classification based on phenology, the most suitable times to separate one crop from another are during the initial and late senescence growth stages. Although only a limited number of images from optimal periods were used in this research for crop classification, they still demonstrated high potential to distinguish crops efficiently. More importantly, crop classification through crop indices using selected images makes the cropland mapping not only simpler and accurate but also provides the possibility of assessing the area for any particular crop using a single relevant crop index. Hao et al. [16] also adopted a similar approach of using images from optimal growth phases rather than the entire cropping season for crop classification and concluded that this approach can accurately classify the crops by evaluating the results in terms of classification certainty, accuracy, and crop separability. Moreover, Li et al. [23] also concluded that using selected images from optimal periods also reduces the processing time for image analysis, which is particularly significant computationally demanding procedures like image segmentation.

In a recent study, object-based image classification (OBIA) was recognized as an effective approach for achieving efficient results of cropland mapping. Ma et al. [26] determined, after careful evaluation of 173 studies, that not only high-resolution imagery but also moderate-resolution imagery, particularly Landsat, were often used in object-based classification successfully. However, errors in the segmentation process of OBIA can produce uncertainties in the results,therefore, the scale of the segmentation is a very critical parameter that needs to be considered [3]. The scale factor directly controls the size of segments and, consequently, field size. In our study, we used the minimum value of scale so that we directly deal with pixels to minimize the possibilities of error due to the segmentation process,however, its value can be optimized through spatial resolution and average field size of the study area [13]. Missing images due to cloud coverage or other technical issues during essential growth stages may cause problems, but this can be addressed by replacing the image of consecutive years during the same time period. Images from a different year may show irregularities in the phenological cycle, but this does not significantly affect the results, particularly in a region where cropping pattern does not change abruptly over time (Q. [23]).

5 Conclusions

In this research, a novel methodology was devised and evaluated for crop type mapping using a composite of multispectral and phenological crop indices, with a focus on improving classification accuracy and simplicity while limiting dataset and user inputs. The approach was applied to Landsat 8 images through a top-down hierarchical object-based image analysis (OBIA) to map major crops of both cropping seasons (wheat, cotton, maize, and rice) along with non-cropping land cover classes (bare soil, water bodies, and built-up areas). The adopted method was validated through independent reference field samples and comparison with crop area data reported by the agriculture department. We found adequate accuracies, which were estimated to be greater than 85% for both validation procedures. The main advantages of the approach included minimal user input, crop phenology (temporal *NDVI*), and simplicity of the procedure. Furthermore, the rule set developed for land cover and crop mapping in OBIA is fully customizable and can be used for subsequent seasons with minimal edits to threshold values defined for each class. This eases the workload and provides the opportunity to reproduce the results, which is not possible in the case of traditional pixel-based supervised and unsupervised classification. The approach would be more effective with Sentinel-2 dataset at 10-m spatial and 3-day temporal resolution. In summary, our research reached out four primary conclusions:

1. Crop classification can be performed efficiently with minimal use of temporal *NDVI* images through crop indices. In our research, the worst classification accuracy reported was only 76% for rice, potatoes, and fodder, as compared to the best individual crop class accuracy of up to 88%.

2. It is possible to use the adopted approach to reproduce crop-type maps for subsequent years with minimal user interaction, reference data, and changes to defined thresholds. This not only reduces the workload but also minimizes extensive fieldwork and resource use.
3. The combination of temporal *NDVI* and multispectral data provides the additional opportunity to separate general classes, e.g., water bodies, built-up areas, and bare land before defining the rule set for crop classification, resulting in more accurate results.
4. The OBIA-based hierarchical classification procedure yields more reliable results by classifying individual classes without affecting the segmentation of other classes that were previously classified accurately.

The adopted approach can also be used efficiently in other applications, such as tree species and forest type mapping, as well as deforestation monitoring.

Author Contribution W.Y. and N.S. were responsible for the study design and data analysis. S.R.A. led the research and was involved in reviewing the manuscript. N.S., A.R., and A.J. provided critical revisions. All authors approved the final version of the manuscript for submission.

Funding Open access funding provided by The Hong Kong Polytechnic University. The research was partly supported by the University Grants Council of the Hong Kong Polytechnic University (P0048214) Hong Kong Special Administrative Region.

Data Availability The data that support the findings of this research are available from the corresponding author, [NS], upon request.

Declarations

Competing interests The authors declare no competing interests.

References

1. Ahmad I, Saeed U, Fahad M, Ullah A, Habib ur Rahman, M., Ahmad, A., & Judge, J. (2018) Yield forecasting of spring maize using remote sensing and crop modeling in Faisalabad-Punjab Pakistan. Journal of the Indian Society of Remote Sensing 46(10):1701–1711. https://doi.org/10.1007/s12524-018-0825-8
2. Belgiu M, Csillik O (2018) Sentinel-2 cropland mapping using pixel-based and object-based time-weighted dynamic time warping analysis. Remote Sens Environ 204:509–523. https://doi.org/10.1016/j.rse.2017.10.005
3. Blaschke T, Hay GJ, Kelly M, Lang S, Hofmann P, Addink E, Queiroz Feitosa R, van der Meer F, van der Werff H, van Coillie F, Tiede D (2014) Geographic object-based image analysis - towards a new paradigm. ISPRS J Photogramm Remote Sens. https://doi.org/10.1016/j.isprsjprs.2013.09.014
4. Boschetti M, Busetto L, Manfron G, Laborte A, Asilo S, Pazhanivelan S & Nelson A (2017) PhenoRice: a method for automatic extraction of spatio-temporal information on rice crops using satellite data time series. Remote Sensing of Environment, 194. https://doi.org/10.1016/j.rse.2017.03.029
5. Chakhar A, Ortega-Terol D, Hernández-López D, Ballesteros R, Ortega JF & Moreno MA (2020). Assessing the accuracy of multiple classification algorithms for crop classification using Landsat-8 and Sentinel-2 data. Remote Sensing, 12(11). https://doi.org/10.3390/rs12111735
6. Chen XL, Zhao HM, Li PX, Yin ZY (2006) Remote sensing image-based analysis of the relationship between urban heat island and land use/cover changes. Remote Sens Environ 104(2):133–146. https://doi.org/10.1016/j.rse.2005.11.016
7. Conrad C, Löw F, Lamers JPA (2017) Mapping and assessing crop diversity in the irrigated Fergana Valley, Uzbekistan. Appl Geogr 86:102–117
8. Deafalla THH, Csaplovics E, & El-Abbas MM (2019) Environmental change impacts and human security in semi-arid region, the case of Nuba Mountains of Sudan. In Human and environmental security in the era of global risks (pp. 187–203). Springer International Publishing. https://doi.org/10.1007/978-3-319-92828-9_10
9. Defourny P, Bontemps S, Bellemans N, Cara C, Dedieu G, Guzzonato E, Hagolle O, Inglada J, Nicola L, Rabaute T, Savinaud M, Udroiu C, Valero S, Bégué A, Dejoux JF, El Harti A, Ezzahar J, Kussul N, Labbassi K, Koetz B (2019). Near real-time agriculture monitoring at national scale at parcel resolution: performance assessment of the Sen2-Agri automated system in various cropping systems around the world. Remote Sensing of Environment, 221, 551–568. https://doi.org/10.1016/j.rse.2018.11.007
10. Duro DC, Franklin SE, Dubé MG (2012) A comparison of pixel-based and object-based image analysis with selected machine learning algorithms for the classification of agricultural landscapes using SPOT-5 HRG imagery. Remote Sens Environ 118:259–272. https://doi.org/10.1016/j.rse.2011.11.020
11. Foody G (2010) Assessing the accuracy of remotely sensed data: principles and practices. Photogram Rec 25(130):204–205. https://doi.org/10.1111/j.1477-9730.2010.00574_2.x
12. Gao Y, Marpu P, Niemeyer I, Runfola DM, Giner NM, Hamill T, Pontius RG (2011) Object-based classification with features extracted by a semi-automatic feature extraction algorithm-SEaTH. Geocarto Int 26(3):211–226. https://doi.org/10.1080/10106049.2011.556754
13. Ghazaryan G, Dubovyk O, Löw F, Lavreniuk M, Kolotii A, Schellberg J, Kussul N (2018) A rule-based approach for crop identification using multi-temporal and multi-sensor phenological metrics. European Journal of Remote Sensing 51(1):511–524. https://doi.org/10.1080/22797254.2018.1455540
14. Gitelson AA, Merzlyak MN (1997) Remote estimation of chlorophyll content in higher plant leaves. Int J Remote Sens 18(12):2691–2697. https://doi.org/10.1080/014311697217558
15. Hao P, Wang L, Niu Z, Aablikim A, Huang N, Xu S, Chen F (2014) The potential of time series merged from Landsat-5 TM and HJ-1 CCD for crop classification: a case study for Bole and

Manas Counties in Xinjiang. China Remote Sensing 6(8):7610–7631. https://doi.org/10.3390/rs6087610

16. Hao P, Zhan Y, Wang L, Niu Z, Shakir M (2015) Feature selection of time series MODIS data for early crop classification using random forest: a case study in Kansas, USA. Remote Sensing 7(5):5347–5369. https://doi.org/10.3390/rs70505347
17. Heupel K, Spengler D, & Itzerott S (2018). A progressive crop-type classification using multitemporal remote sensing data and phenological information. PFG – Journal of Photogrammetry, Remote Sensing and Geoinformation Science, 86(2), 53–69. https://doi.org/10.1007/s41064-018-0050-7
18. Huang Y, CHEN, Z. xin, YU, T., HUANG, X. zhi, & GU, X. fa. (2018) Agricultural remote sensing big data: management and applications. J Integr Agric 17(9):1915–1931. https://doi.org/10.1016/S2095-3119(17)61859-8
19. Jamali A (2021) Improving land use land cover mapping of a neural network with three optimizers of multi-verse optimizer, genetic algorithm, and derivative-free function. The Egyptian Journal of Remote Sensing and Space Science 24(3):373–390. https://doi.org/10.1016/j.ejrs.2020.07.001
20. Khalid U. Bin (2017). Economic analysis of integrated farming systems on farm income. a case study of Sahiwal District, Punjab, Pakistan. International Journal of Management and Economics Invention 3(11):1434–1444. https://doi.org/10.18535/ijmei/v3i11.07
21. Kobayashi N, Tani H, Wang X, Sonobe R (2020) Crop classification using spectral indices derived from Sentinel-2A imagery. Journal of Information and Telecommunication 4(1):67–90. https://doi.org/10.1080/24751839.2019.1694765
22. Kohavi R (1995) A study of cross-validation and bootstrap for accuracy estimation and model selection. *I*JCAI International Joint Conference on Artificial Intelligence, 2(2), 1137–1143. https://dl.acm.org/doi/https://doi.org/10.5555/1643031.1643047
23. Li Q, Wang C, Zhang B, Lu L (2015) Object-based crop classification with Landsat-MODIS enhanced time-series data. Remote Sensing 7(12):16091–16107. https://doi.org/10.3390/rs71215820
24. Li X, Shao G (2014) Object-based land-cover mapping with high resolution aerial photography at a county scale in Midwestern USA. Remote Sensing 6(11):11372–11390. https://doi.org/10.3390/rs61111372
25. Löw F, Duveiller G (2014) Defining the spatial resolution requirements for crop identification using optical remote sensing. Remote Sensing 6(9):9034–9063. https://doi.org/10.3390/rs6099034
26. Ma L, Li M, Ma X, Cheng L, Du P, & Liu Y (2017). A review of supervised object-based land-cover image classification. In ISPRS Journal of Photogrammetry and Remote Sensing (Vol. 130, pp. 277–293). Elsevier B.V. https://doi.org/10.1016/j.isprsjprs.2017.06.001
27. Mahmood T, Usman M, & Conrad C (2025). Selecting relevant features for random forest-based crop type classifications by spatial assessments of backward feature reduction. PFG – Journal of Photogrammetry, Remote Sensing and Geoinformation Science, 1–24. https://doi.org/10.1007/s41064-024-00329-4
28. Murakami T, Ogawa S, Ishitsuka N, Kumagai K, Saito G (2001) Crop discrimination with multitemporal SPOT/HRV data in the Saga Plains. Japan International Journal of Remote Sensing 22(7):1335–1348. https://doi.org/10.1080/01431160151144378
29. Orynbaikyzy A, Gessner U, & Conrad C (2019). Crop type classification using a combination of optical and radar remote sensing data: a review. In International Journal of Remote Sensing (Vol. 40, Issue 17, pp. 6553–6595). Taylor and Francis Ltd. https://doi.org/10.1080/01431161.2019.1569791
30. Pan Z, Huang J, Zhou Q, Wang L, Cheng Y, Zhang H, Blackburn GA, Yan J, Liu J (2015) Mapping crop phenology using NDVI time-series derived from HJ-1 A/B data. Int J Appl Earth Obs Geoinf 34(1):188–197. https://doi.org/10.1016/j.jag.2014.08.011
31. Patel JH, & Oza MP (2014). Deriving crop calendar using NDVI time-series. *I*nternational Archives of the Photogrammetry, Remote Sensing and Spatial Information Sciences - ISPRS Archives, XL–8(1):869–873. https://doi.org/10.5194/isprsarchives-XL-8-869-2014
32. Peña J, Gutiérrez P, Hervás-Martínez C, Six J, Plant R, López-Granados F (2014) Object-based image classification of summer crops with machine learning methods. Remote Sensing 6(6):5019–5041. https://doi.org/10.3390/rs6065019
33. Phiri D, Simwanda M, Nyirenda V, Murayama Y, & Ranagalage M (2020). Decision tree algorithms for developing rulesets for object-based land cover classification. ISPRS International Journal of Geo-Information 2020, Vol. 9, Page 329, 9(5), 329. https://doi.org/10.3390/IJGI9050329
34. Rouse RWH, Haas JAW, Schell JA, & Deering DW (1974). Monitoring vegetation systems in the Great Plains with ERTS (Earth Resources Technology Satellites). Goddard Space Flight Center 3d ERTS-1, 1, 309–317. Available at https://ntrs.nasa.gov/api/citations/19740022614/downloads/19740022614.pdf
35. Shah MAA, Özel G, Chesneau C, Mohsin M, Jamal F, & Bhatti MF (2020). A statistical study of the determinants of rice crop production in Pakistan. Pakistan Journal of Agricultural Research, 33(1):97–105. https://doi.org/10.17582/journal.pjar/2020/33.1.97.105
36. Shrestha B, Ahmad S, & Stephen H (2021). Assessing the relationship between the growth of population and crop area with depletion of groundwater in lower Bari Doab Canal. World Environmental and Water Resources Congress 2021: Planning a Resilient Future along America's Freshwaters - Selected Papers from the World Environmental and Water Resources Congress 2021, 872–887. https://doi.org/10.1061/9780784483466.080
37. Singha M, Wu B, & Zhang M (2016). An object-based paddy rice classification using multi-spectral data and crop phenology in Assam, Northeast India. Remote Sensing, 8(6). https://doi.org/10.3390/rs8060479
38. Tan AA, Shafri HZM, Shaharum NSN (2021) Performance of Sentinel-2A Remote sensing system for urban area mapping in Malaysia via pixel-based and OBIA methods. Trends in Sciences 18(21):38
39. Tatsumi K, Yamashiki Y, Canales Torres MA, Taipe CLR (2015) Crop classification of upland fields using random forest of time-series Landsat 7 ETM+ data. Comput Electron Agric 115:171–179. https://doi.org/10.1016/j.compag.2015.05.001
40. Thomas R, Reed M, Clifton K, Appadurai N, Mills A, Zucca C, Kodsi E, Sircely J, Haddad F, Hagen C, Mapedza E, Woldearegay K, Shalander K, Bellon M, Le Q, Mabikke S, Alexander S, Leu S, Schlingloff S, Quiroz R. (2018). A framework for scaling sustainable land management options. Land Degrad Dev, 1–13. https://doi.org/10.1002/ldr.3080
41. Torbick N, Chowdhury D, Salas W, & Qi J (2017). Monitoring rice agriculture across Myanmar using time series Sentinel-1 assisted by Landsat-8 and PALSAR-2. Remote Sensing, 9(2). https://doi.org/10.3390/rs90201019
42. Tormos T, Kosuth P, Durrieu S, Dupuy S, Villeneuve B, Wasson JG (2012) Object-based image analysis for operational fine-scale regional mapping of land cover within river corridors from multispectral imagery and thematic data. Int J Remote Sens 33(14):4603–4633. https://doi.org/10.1080/01431161.2011.637093
43. Usman M, Liedl R, Shahid MA, Abbas A (2015) Land use/land cover classification and its change detection using multi-temporal MODIS NDVI data. J Geog Sci 25(12):1479–1506. https://doi.org/10.1007/s11442-015-1247-y

44. Wardlow BD, Egbert SL, & Kastens JH (2007) Analysis of time-series MODIS 250 m vegetation index data for crop classification in the U.S. Central Great Plains. Remote Sensing of Environment, 108(3), 290–310. https://doi.org/10.1016/j.rse.2006.11.021
45. Weather Spark. (2021). The Typical Weather Anywhere on Earth. Online, 1–12.
46. Xu H (2006) Modification of normalised difference water index (NDWI) to enhance open water features in remotely sensed imagery. Int J Remote Sens 27(14):3025–3033. https://doi.org/10.1080/01431160600589179
47. Yousaf W, Karim W, Kamran M, Rashid S, Ullah H, Riaz M, Umar M, & Chohan K (2021). A paradigm of GIS and remote sensing for crop water deficit assessment in near real time to improve irrigation distribution plan. Agricultural Water Management, 243(August 2020), 106443. https://doi.org/10.1016/j.agwat.2020.106443
48. Zhai Y, Wang N, Zhang L, Hao L, & Hao C (2020). Automatic crop classification in Northeastern China by improved nonlinear dimensionality reduction for satellite image time series. Remote Sensing, 12(17). https://doi.org/10.3390/RS12172726
49. Zhang H, Li Q, Liu J, Du X, Dong T, McNairn H, Champagne C, Liu M, Shang J (2018) Object-based crop classification using multi-temporal SPOT-5 imagery and textural features with a random forest classifier. Geocarto Int 33(10):1017–1035. https://doi.org/10.1080/10106049.2017.1333533
50. Zheng B, Myint SW, Thenkabail PS, Aggarwal RM (2015) A support vector machine to identify irrigated crop types using time-series Landsat NDVI data. Int J Appl Earth Obs Geoinf 34(1):103–112. https://doi.org/10.1016/j.jag.2014.07.002
51. Zhong L, Hu L, Yu L, Gong P, Biging GS (2016) Automated mapping of soybean and corn using phenology. ISPRS J Photogramm Remote Sens 119:151–164. https://doi.org/10.1016/j.isprsjprs.2016.05.014